

# Heat Transfer Analysis of $TiO_2$ Nanofluid over Unsteady Stretching Surface

Zaffer Elahi\*, Tahira Bibi, Azeem Shahzad

## Abstract

In this article, the flow and heat transfer of electrically conducting  $TiO_2$  nanofluid over a stretching surface is manipulated. The governing equations are converted into a nonlinear system of boundary value problems using suitable transformations. The nonlinear system is then solved numerically for different physical parameters such as, Prandtl, Eckert, Biot, volume fraction, Slip and unsteadiness. Later, graphical simulations of energy profile of different shapes of nanoparticles (NPs) are constructed for these parameters. Moreover, the numerical computation of both skin friction  $C_f$  and Nusselt number  $Nu$  are prepared and discussed in Tables 3-4.

**Keywords:** Thin film; Shape factor; Heat transfer; Convective conditions.

Date of Submission: 20-09-2022

Date of acceptance: 04-10-2022

## I. Introduction

A nanofluid is a suspension of nanoparticles (NPs) (with at least one dimension less than 100nm) in a base fluid, such as water, alcohol, oil, or refrigerant. Nanofluid has attracted a lot of attention in the fields of nanotechnology, thermal engineering, and other applications over the last three decades. Several researchers have revealed quantitative evidence of thermal conductivity increase and better heat transfer performance of various nanofluids. The tendency of NPs to cluster in the suspended state causes nanofluid to be unstable. Because of its high surface activity, the NP suspension tends to agglomerate [1]. Due to its interesting features, nanofluid research has exploded in recent years, and different research groups have contributed significantly to this subject by conducting experimental and theoretical studies on various aspects of nanofluids studied in [2]. More detail on nanofluid and construction of NPs can be found in [3]. Nanofluids have a broader range of uses in thermal energy storage systems for cooling and heat transfer to boost heat transfer rate [4] and thermal energy absorption [5, 6, 7].

The heat transfer performance of the plate heat exchanger has been investigated using different nanofluids ( $CeO_2$ ,  $Al_2O_3$ ,  $TiO_2$ ,  $SiO_2$ ) for various volume flow rates and wide range of concentrations by Sajadi [8]. Vasheghani *et al.* measured the thermal conductivity of micro and nanofluids using hot wire method. They also discussed the enhancement of thermal conductivity and viscosity by adding 3wt.% of  $TiO_2$  (either nano or micro) to engine oil. Alias *et al.* [9] reported the enhancement of thermal conductivity by increasing the concentration of NPs, and

\*zaffer.elahi@uetaxila.edu.pk, Department of Basic Sciences, University of Engineering and Technology, Taxila -47050, Pakistan,

tahirasadiq888@gmail.com, Department of Basic Sciences, University of Engineering and Technology, Taxila -47050, Pakistan.

azeem.shahzad@uetaxila.edu.pk, Department of Basic Sciences, University of Engineering and Technology, Taxila -47050, Pakistan.

temperature because of Brownian motion. Yanni *et al.* [10] investigated three-dimensional numerical nanofluid thermocapillary convection around a gas bubble.

The aim of this article is to manipulate the development of thermal conductivity in  $TiO_2$  nanofluid using different NPs with convective condition.

## Nomenclature

$\kappa_f$	Thermal conductivity of the base fluid	$\rho_f$	Density of the base fluid (water)
$\kappa_{nf}$	Thermal conductivity of the nanofluid	$\rho_{nf}$	Density of nanofluid
$C_p$	Specific heat of fluid	$\mu_f$	Dynamic viscosity of water
$Nu$	Nusselt number	$\mu_{nf}$	Dynamic viscosity of nanofluid
$Re$	Reynolds number	$\nu_f$	Kinematic viscosity of water

$Pr$	Prandtl number	$\nu_{nf}$	Kinematic viscosity of nanofluid
$\alpha_f$	Thermal diffusion of water	$\sigma_{nf}$	Electrical conductivity
$\alpha_{nf}$	Thermal diffusion of nanofluid	$(\rho C_p)_{nf}$	Heat capacity of nanofluid

## II. Modeling of the problem

In this paper,  $TiO_2$ -nanofluid film over a stretching surface is considered. The stretching surface is placed along  $xy$  – plane and  $y$  – axis is taken normal to the surface attached with a slit at  $x = 0$ . The stretching of the surface causes flow along  $x$ – axis with velocity  $U_w = \frac{bx}{1 - \alpha t}$ . The surface temperature  $T_s$  is given by

$$T_s = T_0 - T_r \left( \frac{bx^2}{2\nu_f} \right) (1 - \alpha t)^{-\frac{3}{2}},$$

where  $b$  and  $\alpha$  are dimensional constants.  $T$  is the temperature of the nanofluid, while  $T_r$  represents constant reference temperature with slit temperature  $T_0$  and  $\nu_f$  is the kinematic viscosity of pure fluid. The uniform magnetic field acting normal to the surface is defined by  $B(t) = \frac{B_0}{\sqrt{1 - \alpha t}}$ .

Based on these assumptions, the model is governed by the following equations

$$\frac{\partial u}{\partial x} + \frac{\partial v}{\partial y} = 0, \tag{1}$$

$$\frac{\partial u}{\partial t} + u \frac{\partial u}{\partial x} + v \frac{\partial u}{\partial y} = \frac{\mu_{nf}}{\rho_{nf}} \frac{\partial^2 u}{\partial y^2} - \frac{\sigma_{nf}}{\rho_{nf}} B^2(t)u, \tag{2}$$

$$\frac{\partial T}{\partial t} + u \frac{\partial T}{\partial x} + v \frac{\partial T}{\partial y} = \alpha_{nf} \frac{\partial^2 T}{\partial y^2} + \frac{\mu_{nf}}{\rho_{nf} C_p} \left( \frac{\partial T}{\partial y} \right)^2, \tag{3}$$

with respect to the boundary conditions

$$u = U_w + Av_f \frac{\partial u}{\partial y}, \quad v = 0, \quad -\kappa_{nf} \frac{\partial T}{\partial y} = h_f(T_s - T), \quad \text{at } y = 0, \tag{4}$$

$$u \rightarrow 0, \quad T \rightarrow T_0, \quad \text{as } y \rightarrow \infty, \tag{5}$$

where  $h_f$  is the convective heat transfer coefficient, and  $A$  is the proportionality constant.

In the above system,  $\rho_{nf}, \mu_{nf}, \sigma_{nf}, \alpha_{nf}$  are the density, viscosity, electrical conductivity, and diffusivity of the nanofluid defined in [11], as

$$\begin{aligned} \alpha_{nf} &= \frac{\kappa_{nf}}{(\rho C_p)_{nf}}, \quad \rho_{nf} = (1 - \phi)\rho_f + \phi\rho_s, \quad \mu_{nf} = \mu_f(1 + A_1\phi + A_2\phi^2), \quad \sigma_{nf} = (1 - \phi)\sigma_f + \phi\sigma_s, \\ (\rho C_p)_{nf} &= (1 - \phi)(\rho C_p)_f + \phi(\rho C_p)_s. \end{aligned} \tag{6}$$

and

$$\kappa_{nf} = \kappa_f \left[ \frac{\kappa_s + (m - 1)\kappa_f + (m - 1)(\kappa_s - \kappa_f)\phi}{\kappa_s + (m - 1)\kappa_f - (\kappa_s - \kappa_f)\phi} \right], \tag{7}$$

where  $\phi, A_1, A_2,$  and  $(\rho C_p)_{nf}$  are the volume fraction, thermal conductivity coefficients, and

viscosity enhancement heat capacity, respectively. The thermal conductivity and shape factor of NPs are denoted by  $\kappa_s$  and  $m$ , respectively. The subscripts  $f, nf,$  and  $s$  denote the thermo-physical aspects of the base fluid, nanofluid, and solid NPs. The values of coefficients of viscosity enhancement  $A_1, A_2$  and shape factor  $m$  of multi-shape NPs of  $TiO_2$  nanofluid are listed in Table 1, while Table 2 shows the thermo-physical properties of these NPs.

Table 1: Values of shape factors with viscosity coefficients

Physical parameters	Blade	Particle Brick	Shapes Cylinder	Platelets	Sphere
$A_1$	14.6	1.9	13.5	37.1	2.5
$A_2$	123.3	471.4	904.4	612.6	6.5
$m$	8.26	3.72	4.82	5.72	3.0

Table 2: Thermo-physical properties of base fluid and nanofluids [12]

Physical properties	$\rho$ ( $kgm^{-3}$ )	$C_p$ ( $Jkg^{-1}$ )	$\kappa$ ( $Wm^{-1}K$ )	$\sigma$ ( $Sm^{-1}$ )
$H_2O$	997.1	4179	0.613	5.5
$TiO_2$	4250	686.2	8.9538	0.125

Introducing the similarity transformations, as

$$T = T_0 - T_r \left( \frac{bx^2}{2v_f} \right) (1 - \alpha t)^{\frac{3}{2}} \theta(\eta), \quad \eta = \left( \frac{b}{v_f(1 - \alpha t)} \right)^{\frac{1}{2}}, \quad \psi = \left( \frac{b v_f}{1 - \alpha t} \right)^{\frac{1}{2}} x f(\eta). \quad (8)$$

The continuity equation (1) remains constant, while the PDEs (2–3) and boundary conditions(4–5) have been converted into a system of nonlinear ODEs using the transformation stated in (8), as

$$\epsilon_1 f'''(\eta) - \epsilon_3 M f'(\eta) + \left[ f(\eta) f''(\eta) - f'^2(\eta) - S \left( f'(\eta) + \frac{\eta}{2} f''(\eta) \right) \right] = 0, \quad (9)$$

$$\frac{\epsilon_2}{Pr} \theta''(\eta) + \epsilon_1 Ec f''^2(\eta) + \left[ f(\eta) \theta'(\eta) - 2\theta(\eta) f'(\eta) - \frac{S}{2} (3\theta(\eta) + \eta \theta'(\eta)) \right] = 0, \quad (10)$$

subject to

$$f(0) = 0, \quad f'(0) = 1 + K f''(0), \quad \theta'(0) = -\frac{\kappa_f}{\kappa_{nf}} \gamma (1 - \theta(0)), \quad \text{at } \eta = 0, \\ f' \rightarrow 0, \quad \theta \rightarrow 0, \quad \text{as } \eta \rightarrow \infty, \quad (11)$$

where  $K = A \sqrt{\frac{v_f U_w}{x}}$  and  $\gamma = \frac{h_f}{\kappa_f} \left( \frac{x v_f}{U_w} \right)^{\frac{1}{2}}$  are the respective slip parameter and biot-number.

The Eckert number  $Ec$ , magnetic parameter  $M$ , Prandtl number  $Pr$ , and unsteadiness parameter  $S$  are the dimensionless constants, and symbolically written as

$$Ec = \frac{U_w^2}{C_p (T_s - T)}, \quad M = \frac{\beta_0^2 \sigma_f}{b \rho_{nf}}, \quad Pr = \frac{(\rho C_p)_f v_f}{\kappa_f}, \quad \text{and } S = \frac{\alpha}{b}.$$

The constants  $\epsilon_i, i = 1, \dots, 3$  are defined as

$$\epsilon_1 = \frac{1 + A_1 \phi + A_2 \phi^2}{1 - \phi + \phi \left( \frac{\rho_s}{\rho_f} \right)}, \quad \epsilon_2 = \frac{\left( \frac{\kappa_{nf}}{\kappa_f} \right)}{1 - \phi + \phi \left( \frac{\rho_s}{\rho_f} \right)}, \quad \epsilon_3 = \frac{1 - \phi + \phi \left( \frac{\rho_s}{\rho_f} \right)}{1 - \phi + \phi \left( \frac{\rho_s}{\rho_f} \right)}. \quad (12)$$

The solid volume-fraction and density of the nanofluid are described by  $\phi$  and  $\rho$ . In engineering discipline, the skin friction and Nusselt number both have great interest which are defined by

$$C_f = \frac{\tau_w}{\rho_f U_w^2}, \quad \text{and} \quad Nu = \frac{x q_w}{\kappa_f (T_s - T_0)},$$

where

$$\tau_w = \mu_{nf} \left( \frac{\partial u}{\partial y} \right)_{y=0} \quad \text{and} \quad q_w = -\kappa_{nf} \left( \frac{\partial T}{\partial y} \right)_{y=0}. \quad (13)$$

The Eqn. (13) can be represented in non-dimensional form, as

$$Re^{\frac{1}{2}} C_f = (1 + A_1 \phi + A_2 \phi^2) f''(0), \quad \text{and} \quad Re^{-\frac{1}{2}} Nu = -\frac{\kappa_{nf}}{\kappa_f} \theta'(0). \quad (14)$$

### III. Solution methodology

Initially, the nonlinear system (9-11) is converted into a system of first-order equations with the following assumptions

$$y_1 = f, \quad (15)$$

$$y_1' = y_2, \quad (16)$$

$$y_2 = y_3, \quad (17)$$

$$y_3' = \epsilon_1^{-1} \left[ \epsilon_3 M y_2 - y_1 y_3 + y_2^2 + S \left( y_2 + \frac{\eta}{2} y_3 \right) \right], \quad (18)$$

$$\theta = y_4, \quad (19)$$

$$y_4' = y_5 \quad (20)$$

$$y_5' = Pr \epsilon_2^{-1} \left[ -Ec \epsilon_1 y_3^2 - y_1 y_5 + 2 y_2 y_4 + \frac{S}{2} (3y_4 + \eta y_5) \right], \quad (21)$$

$$y_1(0) = 0, \quad y_2(0) = 1 + K y_3(0), \quad y_5(0) = -\frac{\kappa_f}{\kappa_{nf}} \gamma (1 - y_4(0)), \quad \text{at } \eta = 0, \quad (22)$$

$$y_2 \rightarrow 0, \quad y_4 \rightarrow 0, \quad \text{as } \eta \rightarrow \infty, \quad (23)$$

The above first-order system of equations is then solved on Matlab using numerical technique “**BVP4C**”.

### IV. Results interpretation

The interpretation of obtained results have been discussed in this section. Further, variation in shape of NPs of *TiO<sub>2</sub>* nanofluid over a stretching surface has also been studied for both velocity and temperature fields in the following subsections.

#### 4.1 Velocity field

Figure 1 shows the effect of multi-shape NPs of *TiO<sub>2</sub>* nanofluids keeping other physical parameters fixed. It is clearly seen that a drastic change is observed in velocity field while changing shapes of NPs. It should be noted that the velocity is high for platelet shape, and low at spherical shape NPs.

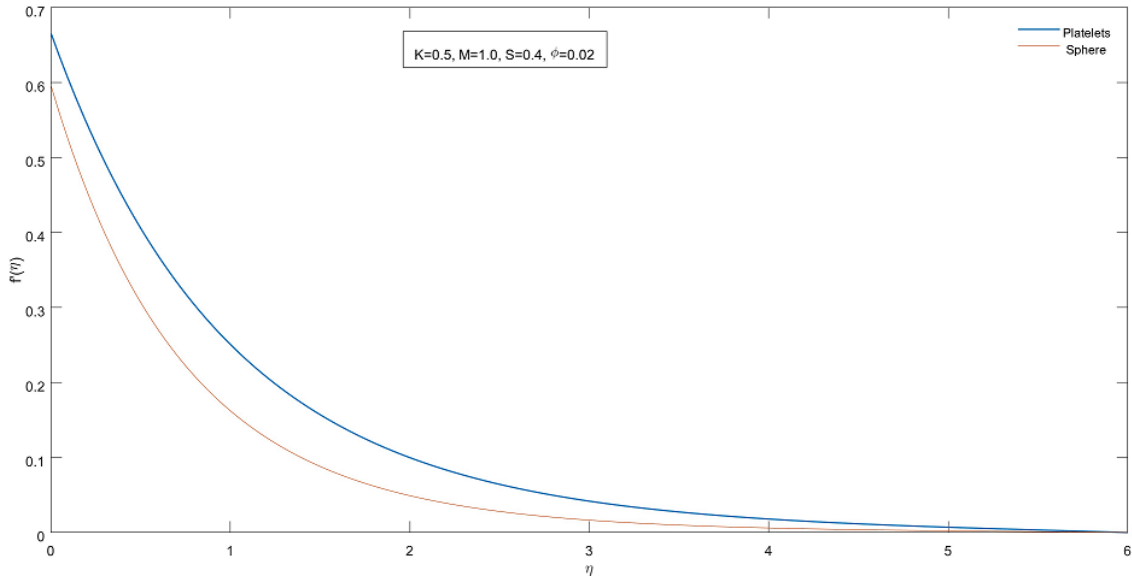


Figure 1: Effect of shape factor of NPs on velocity field

4.2 Temperature field

The effect of slip parameter  $K$  on temperature field distribution is plotted in Figure 2(a-b) that indicates the decay in temperature at different values of  $K$ . While in the case of volume-fraction parameter  $\phi$ , the temperature field is getting increased for platelet shape NPs, but the opposite trend is seen for spherical shape NPs as shown in Figure 3(a-b). Figure 4 (a-b) elucidates that the temperature field effected prominently for growing values of biot-number  $\gamma$ . Figure 5(a-b) represents the impact of the Eckert number on the temperature field. By increasing the value of Eckert number, the temperature field getting higher. But in the case of Prandtl number, the temperature field reduces near the surface, whereas the opposite trend occurs near the free surface as shown in Figure 6(a-b). Finally, the effect of shape factor on temperature field are quite strong for platelet shape and low for spherical shape NPs, in Figure 7. Particularly, for multi-shape NPs, the dimensionless shear stress at the surface is calculated and summarized in Table 3. The skin friction coefficient rises for magnetic  $M$  and unsteadiness  $S$  parameters, while the opposite is seen in the case of slip  $K$  and volume fraction parameters  $\phi$ .

Table 3: Numerical values of skin friction

$K$	Physical parameters $\phi$	$M$	$S$	Platelet $-Re^{\frac{1}{2}} C_f$	Sphere
0.5	--	--	--	0.66871951	0.80766488
1.0	--	--	--	0.49044125	0.56410362
1.5	--	--	--	0.38940407	0.43586071
--	<b>0.02</b>	--	--	0.66871951	0.80766488
--	<b>0.04</b>	--	--	0.56435350	0.80008536
--	<b>0.06</b>	--	--	0.48367517	0.79208929
--	--	<b>0.5</b>	--	0.61187959	0.74350633
--	--	<b>1.0</b>	--	0.66871951	0.80766488
--	--	<b>2.0</b>	--	0.75641958	0.90384095
0.5	0.02	1.0	<b>0.4</b>	0.66871951	0.80766488
--	--	--	<b>0.6</b>	0.68507079	0.82588767
--	--	--	<b>0.8</b>	0.70065034	0.84313550

Table 4 gives numerical results for heat transfer coefficients at the surface. It is obvious that increasing both the Prandtl- and Eckert-numbers gradually reduces the Nusselt number, whereas the rise in other physical parameters results the increase in Nusselt value.

Table 4: Numerical values of Nusselt number

Physical parameters						Platelet	Sphere
$K$	$\phi$	$Ec$	$S$	$Pr$	$\gamma$	$Re^{-\frac{1}{2}} Nu$	
0.0	0.02	1.0	0.4	6.0	0.1	0.041573534	0.046972874
0.5	--	--	--	--	--	0.069456143	0.076476894
1.0	--	--	--	--	--	0.079386332	0.084760810
<b>0.5</b>	<b>0.00</b>	1.0	0.4	6.0	0.1	0.075735930	0.075735930
--	<b>0.02</b>	--	--	--	--	0.069456143	0.076476894

--	<b>0.04</b>	--	--	--	--	0.064506794	0.077090813
<b>0.5</b>	0.02	<b>0.0</b>	1.0	0.4	6.0	0.097035480	0.096898433
--	--	<b>0.5</b>	--	--	--	0.083245811	0.086687663
--	--	<b>1.0</b>	--	--	--	0.069456143	0.076476894
<b>0.5</b>	0.02	--	<b>0.4</b>	6.0	0.1	0.069456143	0.076476894
--	--	--	<b>0.6</b>	--	--	0.071838482	0.078550290
--	--	--	<b>0.8</b>	--	--	0.073740496	0.080176809
<b>0.5</b>	0.02	1.0	0.4	<b>4.0</b>	0.1	0.070815276	0.077512326
--	--	--	--	<b>6.0</b>	--	0.069456143	0.076476894
--	--	--	--	<b>8.0</b>	--	0.068473325	0.075677514
<b>0.5</b>	0.02	1.0	0.4	6.0	<b>0.2</b>	0.134912770	0.148352530
--	--	--	--	--	<b>0.4</b>	0.255134070	0.279866810
--	--	--	--	--	<b>0.6</b>	0.362939750	0.397255620

### V. Conclusion

Effects of multi-shape NPs on electrically conducting  $TiO_2$  nanofluids over exponentially stretching surface have been investigated, numerically. The influence of the pertinent parameters on velocity and temperature fields have been displayed graphically and discussed, in detail. The findings of the present study are, as under

- An increment in slip parameter  $K$  results in decay of skin friction value.
- The velocity and thermal conductivity of  $TiO_2$  nanofluid is maximum at platelet shape, and minimum at spherical shape NPs.
- The temperature profile has been increased by increasing the biot-number ( $\gamma$ ).
- The skin friction coefficient is getting decreased for slip and volume fraction parameters, while increased at magnetic-and unsteadiness-parameters.
- The Nusselt number is getting increased for slip, unsteadiness, and biot number at both Platelet and spherical shape NPs.
- By Changing the value of Prandtl-and Eckert-numbers yield the decrease in Nusselt number, while the opposite trend is seen in the case of volume fraction parameter.

### References

- [1]. S. Chakraborty and P. K. Panigrahi, "Stability of nanofluid: A review," Applied Thermal Engineering, vol. 174, p. 115259, 2020.
- [2]. S. M. Iqbal, M. Arulprakasajothi, N. D. Raja, S. M. J. Bosko, and M. B. Teja, "Investigation on the thermal behaviour of titanium dioxide nanofluid," Materials Today: Proceedings, vol. 5, no. 9, pp. 20608–20613, 2018.
- [3]. H. Alias and M. F. C. Ani, "Thermal characteristic of nanofluids containing titaniumdioxide nanoparticles in ethylene glycol," Chemical Engineering Transactions, vol. 56, pp. 1459–1464, 2017.
- [4]. S. Lohrasbi, S. Z. Miry, M. Gorji-Bandpy, and D. D. Ganji, "Performance enhancement of finned heat pipe assisted latent heat thermal energy storage system in the presence of nano-enhanced  $H_2O$  as phase change material," International Journal of Hydrogen Energy, vol. 42, no. 10, pp. 6526–6546, 2017.
- [5]. S. Z. Miry, M. Roshani, P. Hanafizadeh, M. Ashjaee, and F. Amini, "Heat transfer and hydrodynamic performance analysis of a miniature tangential heat sink using  $Al_2O_3 - H_2O$  and  $TiO_2 - H_2O$  nanofluids," Experimental Heat Transfer, vol. 29, no. 4, pp. 536–560, 2016.
- [6]. S. Z. Miry, S. Lohrasbi, H. Irani, M. Ashjaee, and D. D. Ganji, "Thermal energy absorption in a heat sink with elliptical cross section and tangential impinging inlet flow of nanofluid," Experimental Thermal and Fluid Science, vol. 89, pp. 50–61, 2017.
- [7]. M. Roshani, S. Ziaeddin M., P. Hanafizadeh, and M. Ashjaee, "Hydrodynamics and heat transfer characteristics of a miniature plate pin-fin heat sink utilizing  $Al_2O_3 - water$  and  $TiO_2 - water$  nanofluids," Journal of Thermal Science and Engineering Applications, vol. 7, no. 3, p. 031007, 2015.
- [8]. A. R. Sajadi and M. H. Kazemi, "Investigation of turbulent convective heat transfer and pressure drop of  $TiO_2/water$  nanofluid in circular tube," International Communications in Heat and Mass Transfer, vol. 38, no. 10, pp. 1474–1478, 2011.
- [9]. H. Alias and M. F. C. Ani, "Thermal characteristic of nanofluids containing titaniumdioxide nanoparticles in ethylene glycol," Chemical Engineering Transactions, vol. 56, pp. 1459–1464, 2017.
- [10]. Y. Jiang, X. Zhou, and Y. Wang, "Effects of nanoparticle shapes on heat and mass transfer of nanofluid thermocapillary convection around a gas bubble," Microgravity Science and Technology, vol. 32, no. 2, pp. 167–177, 2020.
- [11]. H. C. Brinkman, "The viscosity of concentrated suspensions and solutions," The Journal of chemical physics, vol. 20, no. 4, pp. 571–571, 1952.
- [12]. M. Gupta, V. Singh, S. Kumar, S. Kumar, N. Dilbaghi, and Z. Said, "Up to date review on the synthesis and thermophysical properties of hybrid nanofluids," Journal of cleaner production, vol. 190, pp. 169–192, 2018.

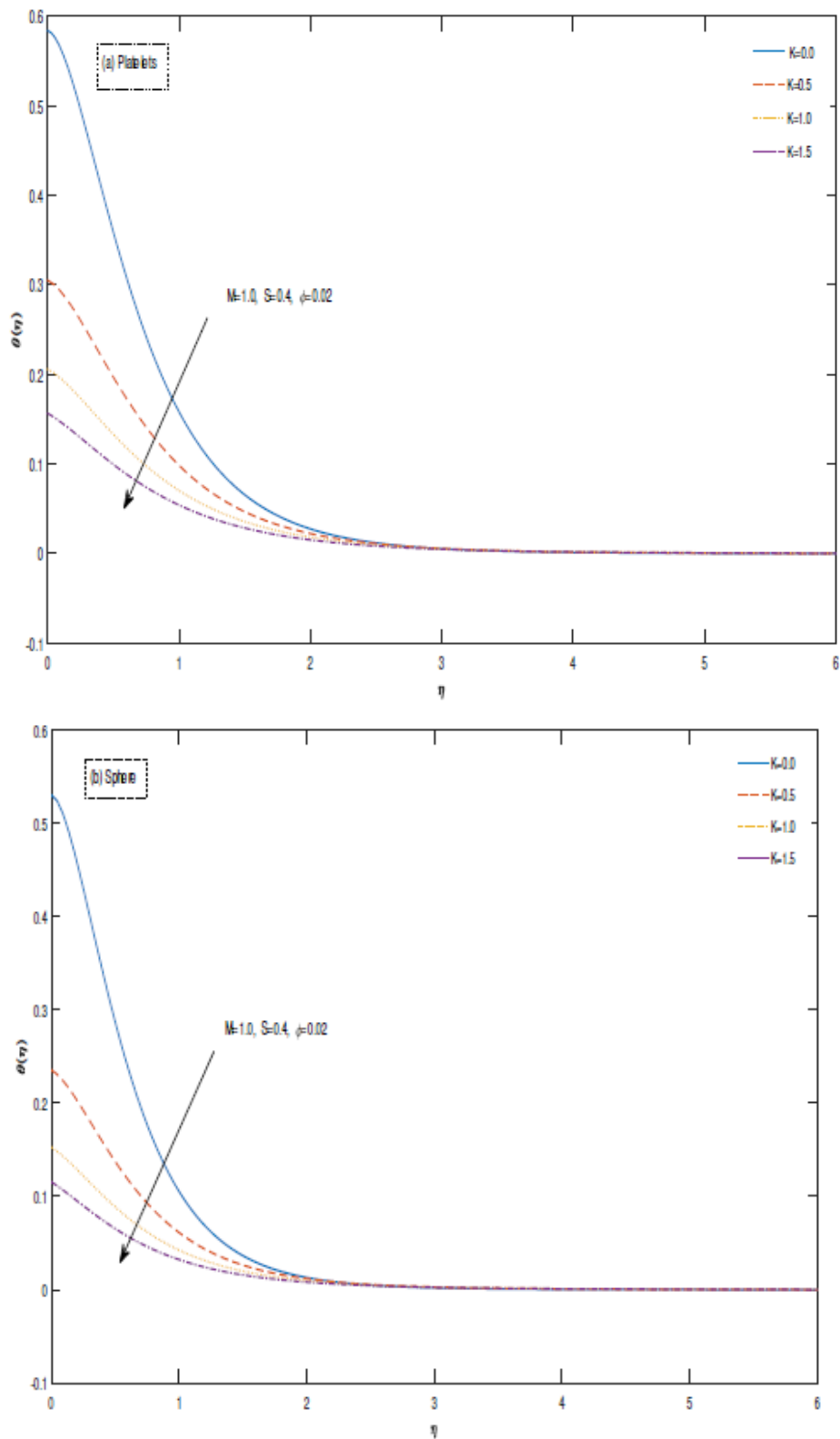


Figure 2: Effect of temperature profile changing slip  $K$

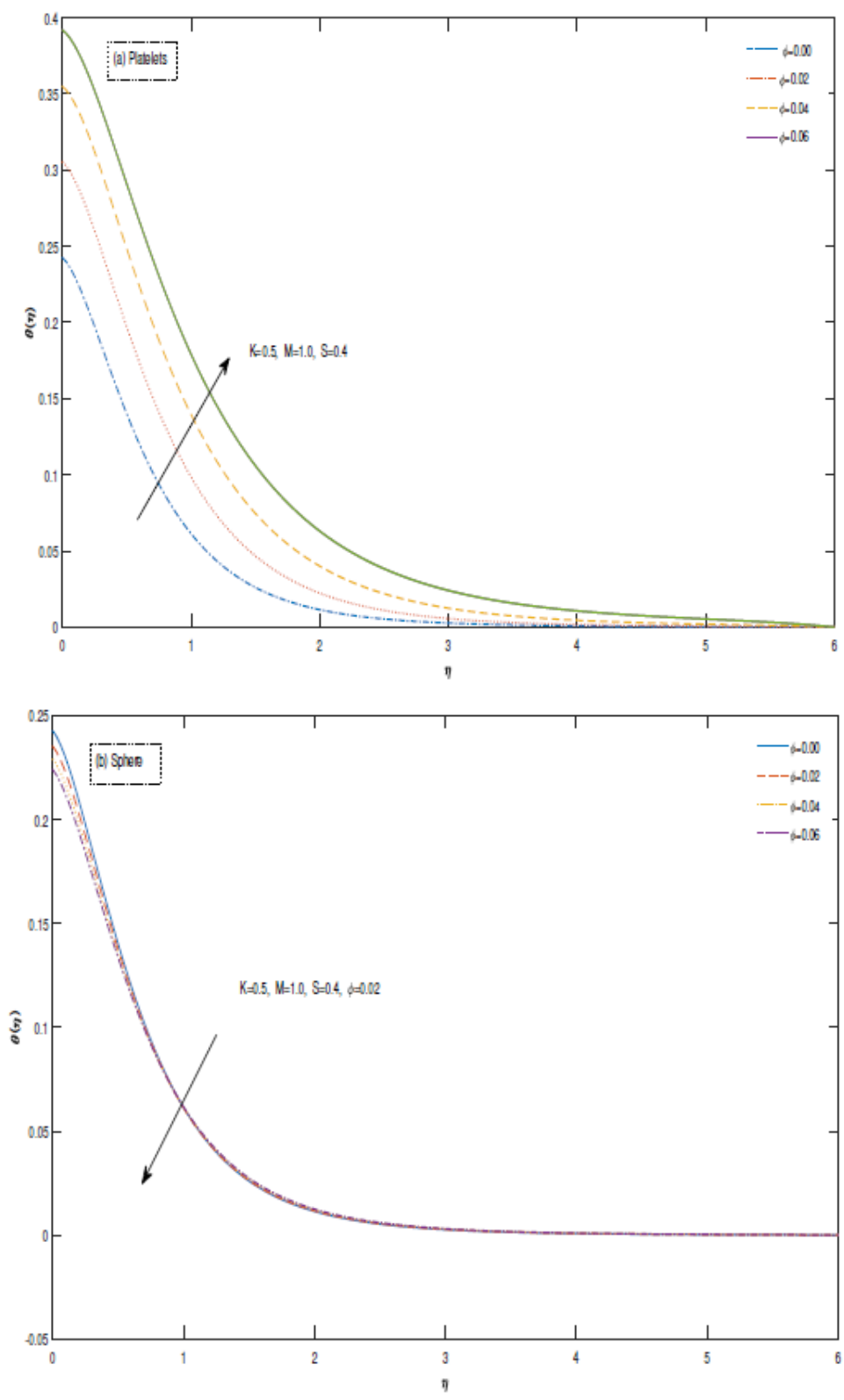


Figure 3: Effect of temperature profile changing volume fraction  $\phi$

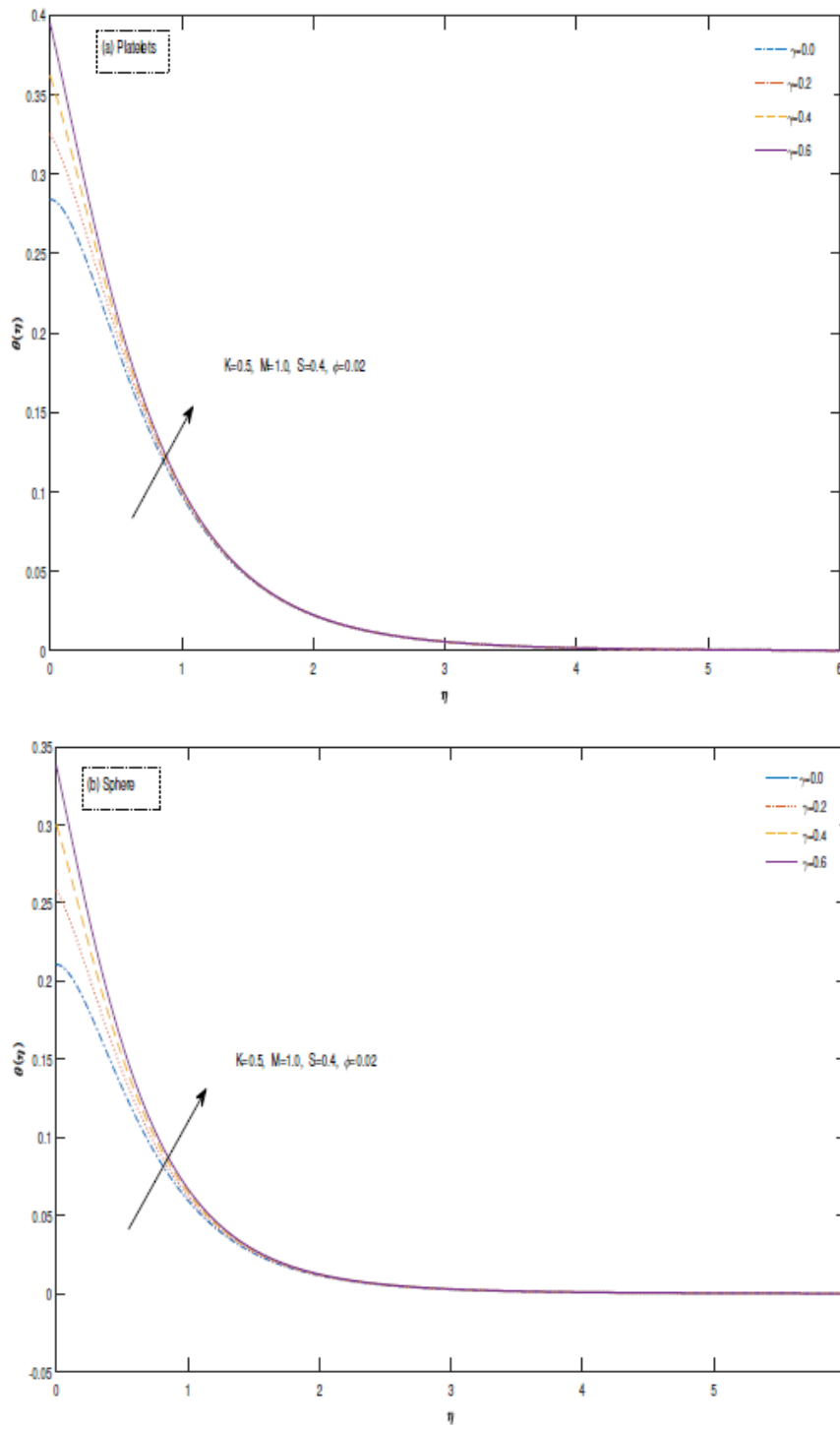


Figure 4: Effect of temperature profile changing biot  $\gamma$



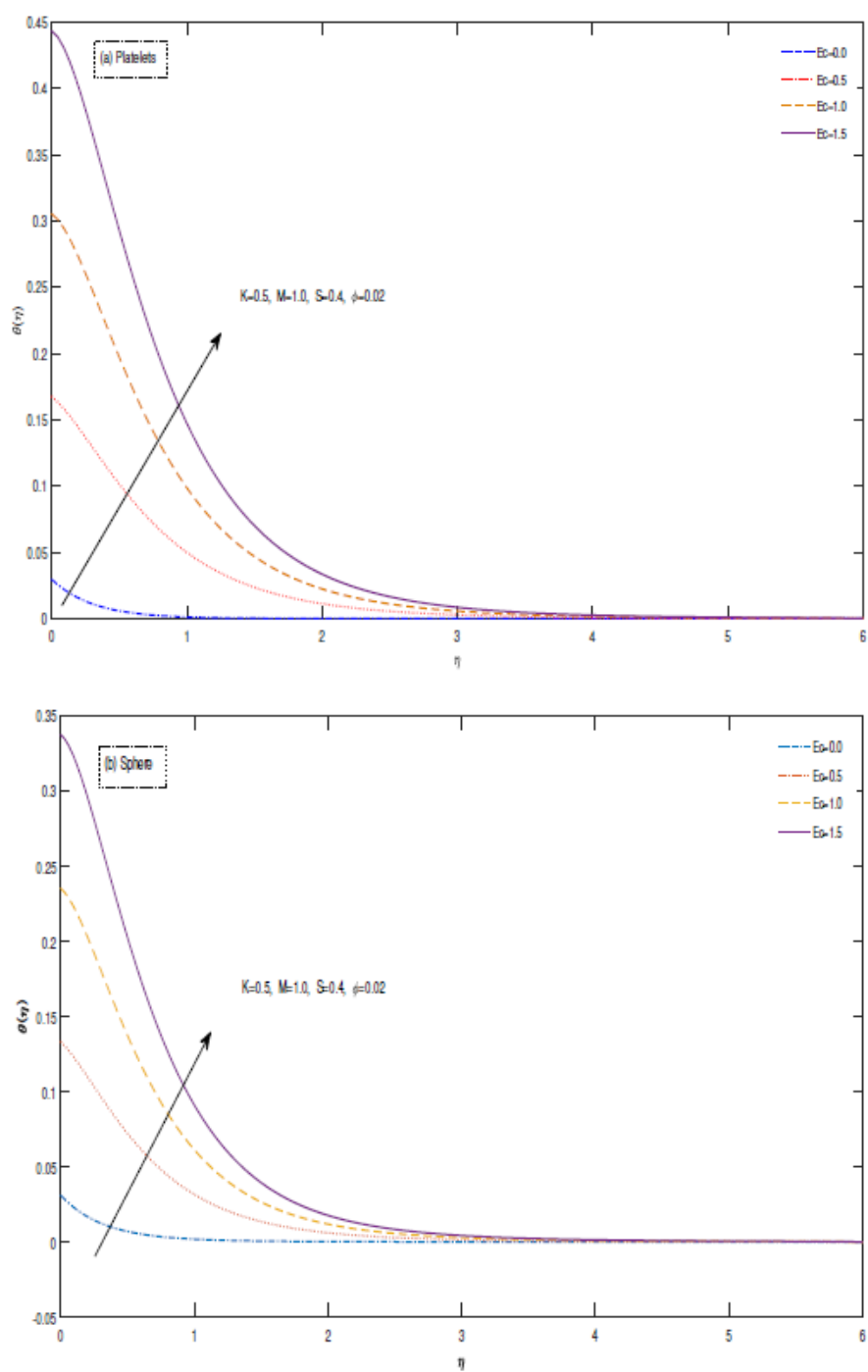


Figure 5: Effect of temperature profile changing Eckert  $Ec$

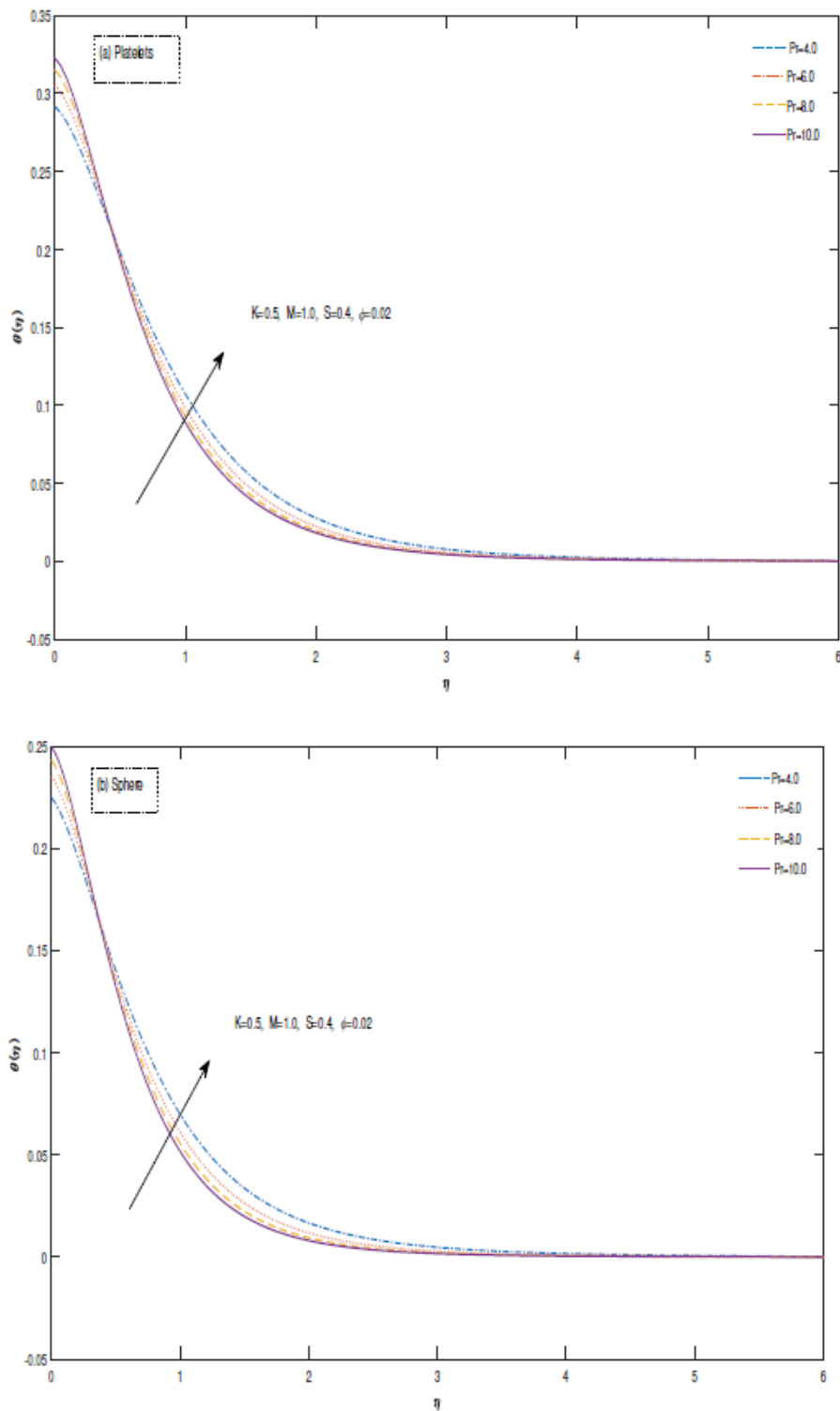


Figure 6: Effect of temperature profile changing Prandtl  $Pr$

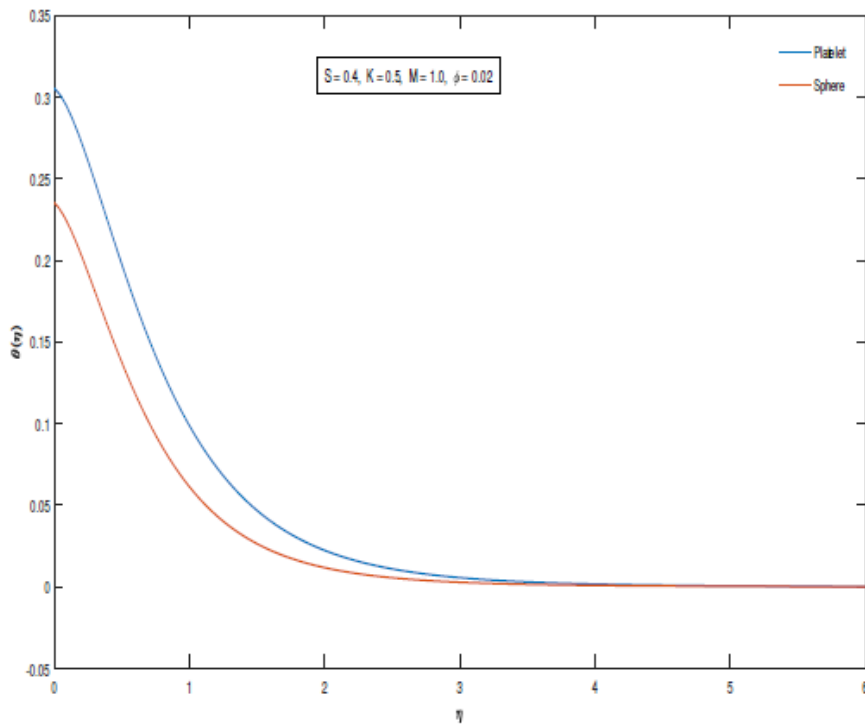


Figure 7: Effect of shape factor of NPs on Temperature field